Electronic Supplementary Material (ESI) for Inorganic Chemistry Frontiers.

Supporting information for

The Influence of NCE^- (E = S, Se, BH_3) Ligands on the Temperature of Spin Crossover in a Family of Iron(II) Mononuclear Complexes

Bin Fei,[a] Xiu Qin Chen,[a] You De Cai,[a] Jing Kun Fang,[a] Ming Liang Tong,[c] Jiri Tucek [d] and Xin Bao,*[a,b]

a. School of Chemical Engineering, Nanjing University of Science and Technology, 210094 Nanjing, P. R. China.

b. State Key Laboratory of Coordination Chemistry, Coordination Chemistry Institute, School of Chemistry and Chemical Engineering, Nanjing University, Nanjing 210093, P. R. China

c. Key Laboratory of Bioinorganic and Synthetic Chemistry of Ministry of Education, School of Chemistry and Chemical Engineering, Sun Yat-Sen University, 510275 Guangzhou, P. R. China.

d. Regional Centre of Advanced Technologies and Materials, Department of Experimental Physics, Faculty of Science, Palacky University, Slechtitelu 11, 78371 Olomouc, Czech Republic.

Table S1. Crystal data and refinement details

	$[FeL_{Cl}(NCS)_2]$ (**1-S**)	$[FeL_{Cl}(NCSe)_2]$ (**1-Se**)		$[FeL_{Cl}(NCBH_3)_2]$ (**1-BH$_3$**)	
Temperature / K	123	123	298	123	298
Spin state	HS	LS	HS	LS	HS
Empirical formula	$C_{16}H_{16}Cl_2FeN_6S_2$	$C_{16}H_{16}Cl_2FeN_6Se_2$	$C_{16}H_{16}Cl_2FeN_6Se_2$	$C_{16}H_{22}B_2Cl_2FeN_6$	$C_{16}H_{22}B_2Cl_2FeN_6$
Formula weight / g mol^{-1}	483.22	577.02	577.02	446.76	446.76
Crystal system	Orthorhombic	Orthorhombic	Orthorhombic	Orthorhombic	Orthorhombic
Space group	Pbcn	Pbcn	Pbcn	Pbcn	Pbcn
a / Å	16.1129(14)	15.931(12)	16.384(6)	15.1811(6)	15.9885(7)
b / Å	9.5488(7)	9.285(7)	9.657(3)	9.6182(4)	9.8134(5)
c / Å	13.0274(9)	13.394(10)	13.344(4)	13.8167(6)	13.5420(7)
Volume / Å^3	2004.4(3)	1981(2)	2111.3(12)	2016.31(15)	2124.76(18)
Z	4	4	4	4	4
ρ_{calc} / mg mm^{-3}	1.601	1.935	1.815	1.472	1.397
μ / mm^{-1}	1.242	4.72	4.429	1.027	0.974
F(000)	984	1128	1128	920	920
Reflections collected	13936	28617	25370	78861	73854
Independent reflections	2045	2471	1901	2334	2459
R_{int}	R_{int} = 0.0951	R_{int} = 0.0810	R_{int} = 0.1034	R_{int} = 0.0867	R_{int} = 0.1130
Goodness-of-fit on F^2	1.062	1.022	1.035	1.083	1.026
Final R indexes[a] [$I \geq 2\sigma(I)$]	R_1 = 0.0429 wR_2 = 0.0602	R_1 = 0.0326 wR_2 = 0.0525	R_1 = 0.0361 wR_2 = 0.0583	R_1 = 0.0346 wR_2 = 0.0719	R_1 = 0.0400 wR_2 = 0.0790
Final R indexes [all data]	R_1 = 0.0917 wR_2 = 0.0709	R1 = 0.0565 wR2 = 0.0568	R_1 = 0.0680 wR_2 = 0.0664	R_1 = 0.0473 wR_2 = 0.0754	R_1 = 0.0744 wR_2 = 0.0907
Largest diff. peak/hole / eÅ^{-3}	0.41/-0.51	0.49/-0.54	0.39/-0.40	0.73/-0.30	0.40/-0.37

Table S2. Selected bond lengths and structural parameters for **1**.

$[FeL_{Cl}(NCS)_2]$ (**1-S**)		$[FeL_{Cl}(NCSe)_2]$ (**1-Se**)		$[FeL_{Cl}(NCBH_3)_2]$ (**1-BH$_3$**)	
***T* / K**	123	123	298	123	298
Spin state	HS	LS	HS	LS	HS
Fe-N_{NCX} / Å	2.093(3)	1.934(3)	2.094(4)	1.940(16)	2.114(2)
Fe-$N_{pyridine}$ / Å	2.189(2)	1.979(3)	2.192(3)	1.966(16)	2.1871(19)
Fe-N_{amine} / Å	2.240(2)	2.017(2)	2.226 (3)	2.014(16)	2.224(2)
Fe-$N_{average}$ / Å	2.17	1.98	2.17	1.97	2.18
***cis* N−Fe−N / º**	74.70(9)-101.14(15)	80.15(10)-98.01(10)	74.82(12)-100.92(12)	83.49 (7)-95.60(6)	75.14(7)-101.64(7)
***trans* N−Fe−N / º**	163.56(9)-174.28(13)	173.29(9)-177.54(13)	164.22(14)-174.63(17)	174.58(9)-176.66(7)	164.45(8)-175.96(10)
Σ_{Fe} / º	88.3(5)	60.4(6)	86.8(7)	42.7(4)	89.5(4)
Θ	245.0(11)	169.1(11)	238.8(11)	110.4(8)	241.7(9)
N-C-S / º	178.6(3)	178.5(2)	178.5(4)	178.5(2)	178.7(3)
Fe-N-C_{NCS} / º	162.6(2)	173.6(2)	163.9(4)	172.43(16)	165.7(2)

Table S3. Selected supramolecular interactions in **1-E** (E=S, Se, BH_3).

	123K		**298K**	
1-S	Cl1-S1	3.372(13)		
	H2-S1	2.6403(9)		
1-Se	Cl1-Se1	3.459(3)	Cl1-Se1	3.529(16)
	H2-Se1	2.585(13)	H2-Se1	2.7465(8)
1-BH$_3$	Cl3-B1	3.454(2)	Cl1-B1	3.549(3)

H2-B1	3.129(2)	H2-B1	2.969(3)

Table S4. Values of the Mössbauer hyperfine parameters, derived from the least-square fitting of the ^{57}Fe Mössbauer spectra, where T is the temperature of the measurement, δ is the isomer shift, ΔE_Q is the quadrupole splitting, Γ is the linewidth, and RA is the spectral area of individual spectral components identified during spectra fitting.

Sample	T (K)	Component	δ ± 0.01 (mm/s)	ΔE_Q ± 0.01 (mm/s)	Γ ± 0.01 (mm/s)	RA ± 1 (%)	Assignment
1-S	80	Doublet	1.11	1.79	0.27	100	Fe(II), S = 2
	300	Doublet	0.99	1.36	0.24	100	Fe(II), S = 2
1-Se	80	Doublet	0.50	0.19	0.28	100	Fe(II), S = 0
	300	Doublet	0.98	1.23	0.26	100	Fe(II), S = 2
1-BH_3	80	Doublet	0.47	0.17	0.27	100	Fe(II), S = 0
	300	Doublet	0.98	0.97	0.25	100	Fe(II), S = 2

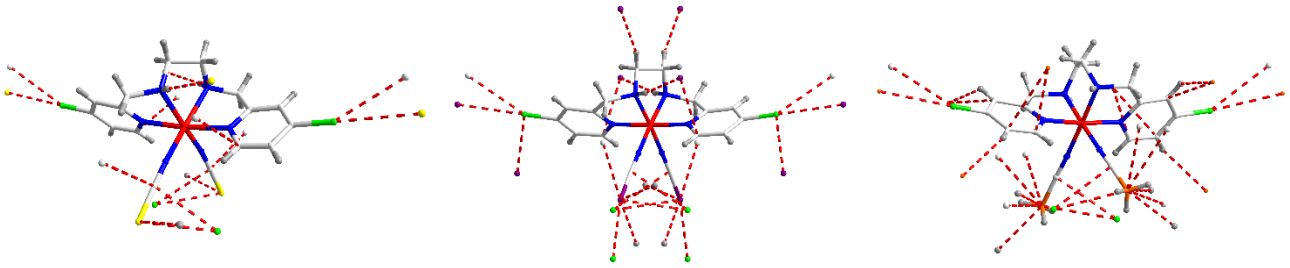

Fig. S1 Intermolecular interactions exhibited by an Fe(II) complex with neighboring molecules in **1-S** (left), **1-Se** (middle) and **1-BH$_3$** (right).

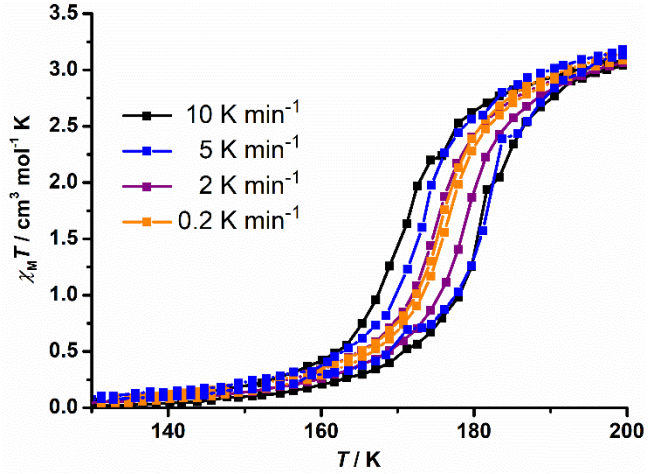

Fig. S2 Scan rate dependent hysteresis loops of $\chi_M T$-T curves for **1-Se**.

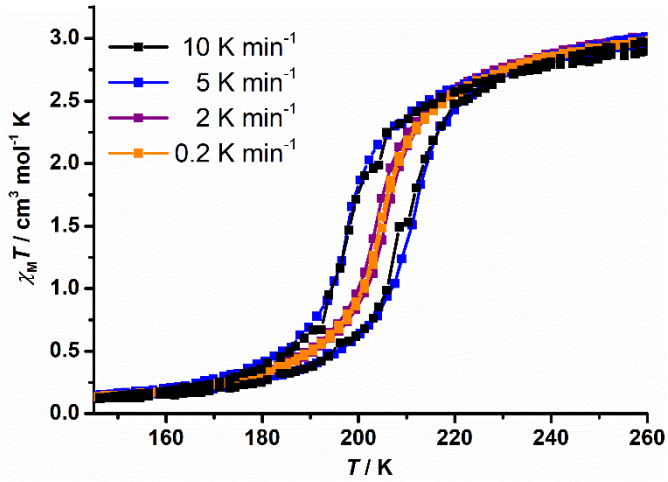

Fig. S3 Scan rate dependent hysteresis loops of $\chi_M T$-T curves for **1-BH$_3$**.

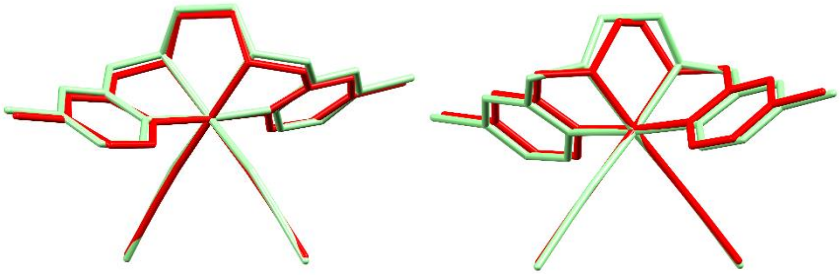

Fig. S4 Overlay of the molecular structures of the Fe(II) complex at 123 K (LS state) and 298 K (HS state) in **1-Se** (left) and **1-BH$_3$** (right).

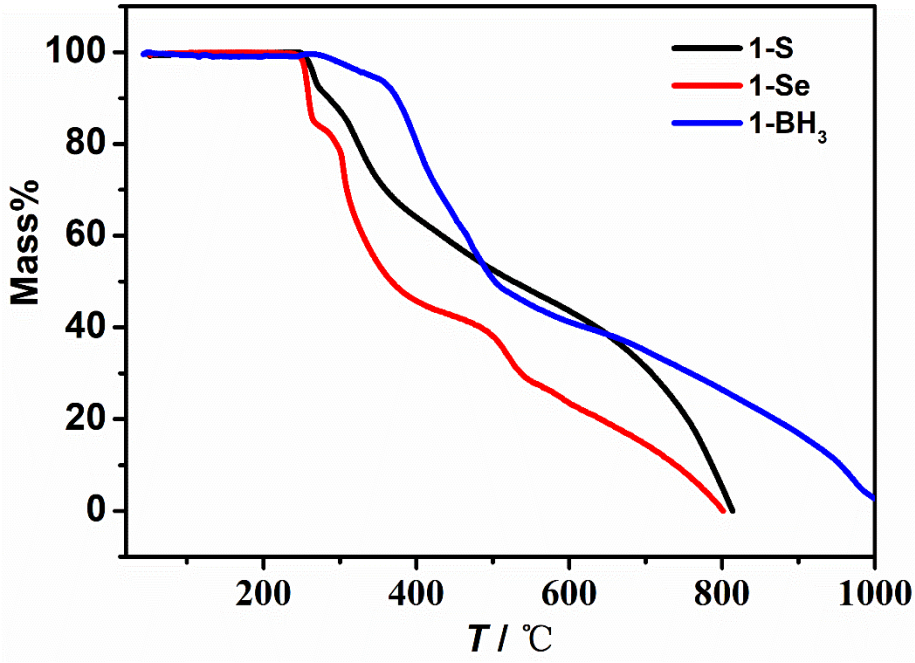

Fig. S5 Thermogravimetric analysis (TGA) curves for **1-E** (E=S, Se, BH_3) at a 10 K min^{-1} temperature rate under N_2 atmosphere.

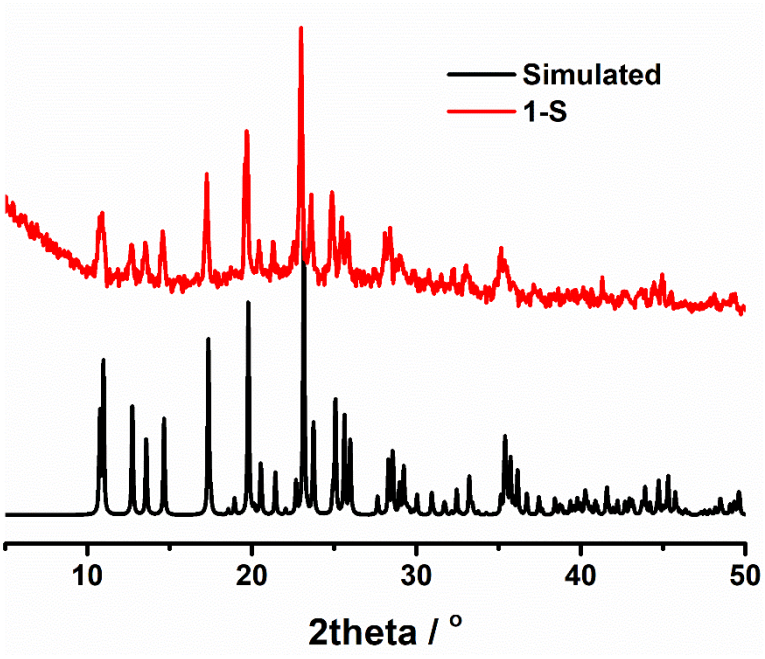

Fig. S6 Experimental and simulated PXRD patterns of **1-S**.

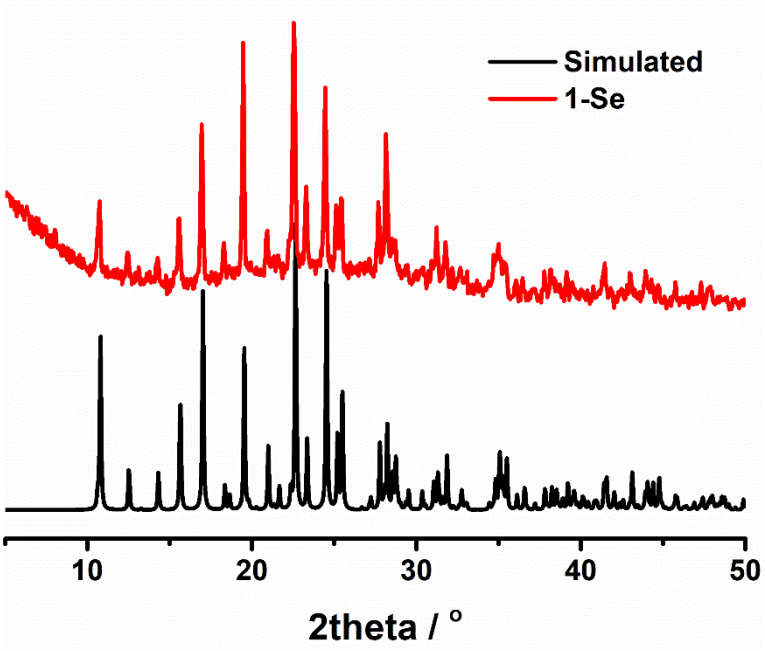

Fig. S7 Experimental and simulated PXRD patterns of **1-Se**.

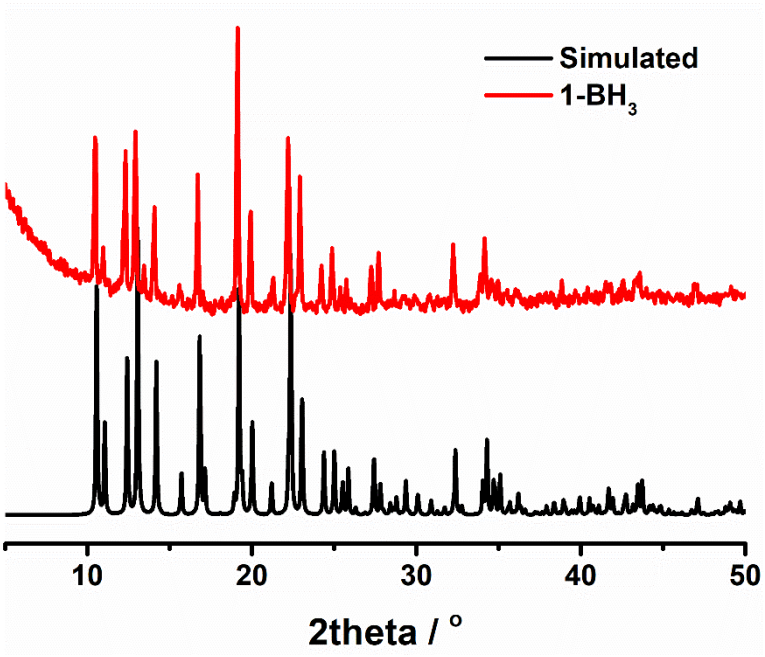

Fig. S8 Experimental and simulated PXRD patterns of **1-BH$_3$**.